Eur. Phys. J. C (2022) 82:845
https://doi.org/10.1140/epjc/s10052-022-10803-1

THE EUROPEAN PHYSICAL JOURNAL C

Regular Article - Theoretical Physics

Search for noncommutative interactions in $\gamma\gamma \to \gamma\gamma$ process at the LHC

S. C. İnan[1,a], **A. V. Kisselev**[2,b]

[1] Department of Physics, Sivas Cumhuriyet University, 58140 Sivas, Turkey
[2] Division of Theoretical Physics, A.A. Logunov Institute for High Energy Physics, NRC "Kurchatov Institute", 142281 Protvino, Russia

Received: 14 June 2022 / Accepted: 14 September 2022 / Published online: 28 September 2022

Abstract The noncommutative QED (NCQED) has a non-Abelian nature due to the presence of 3- and 4-photon vertices in the lagrangian. Thus, NCQED predicts a new physics contribution to the $\gamma\gamma \to \gamma\gamma$ scattering already at the tree level. We have examined NCQED by studying the light-by-light process at the 14 TeV LHC with intact protons. Our results show that the NC scale up to $\Lambda_{\mathrm{NC}} = 1.64(1.35)$ TeV can be probed in the $pp \to p(\gamma\gamma)p \to p'(\gamma\gamma)p'$ collision for the time-space (space-space) NC parameters. These bounds are stronger than the limits that can be obtained in the light-by-light scattering at high energy linear colliders.

1 Introduction

The quantization of the electromagnetic field in a noncommutative (NC) space-time has a long story [1,2]. To a large extent, an interest in NC quantum field theories [3–5] was mainly motivated by string theory [6–9]. In NC field theories the conventional coordinates are represented by noncommutative operators,

$$[\hat{X}_\mu, \hat{X}_\nu] = i\theta_{\mu\nu}, \tag{1}$$

where $\theta_{\mu\nu}$ is the NC *constant* of dimension (mass)$^{-2}$. In what follows,

$$\theta_{\mu\nu} = \frac{c_{\mu\nu}}{\Lambda_{\mathrm{NC}}^2}, \tag{2}$$

where the dimensionless elements of the antisymmetric matrix $c_{\mu\nu}$ are assumed to be of order unity.

Let the field $\hat{\Phi}(\hat{X})$ be an element of the algebra (1). The noncommutativity of the space-time can be implemented by the *Weyl–Moyal correspondence* [10–14]

$$\hat{\Phi}(\hat{X}) = \frac{1}{(2\pi)^2}\int d^4x\, e^{ik\hat{X}}\phi(k),$$
$$\phi(k) = \frac{1}{(2\pi)^2}\int d^4k\, e^{-ikx}\,\Phi(x), \tag{3}$$

where k, x are real variables. Thus, we associate $\hat{\Phi}(\hat{X})$ with a function of classical variable x. As it follows from (3),

$$\hat{\Phi}_1(\hat{X})\hat{\Phi}_2(\hat{X}) = \frac{1}{(2\pi)^4}\int d^4k\, d^4p\, e^{ik\hat{X}}\phi(k)\, e^{ip\hat{X}}\phi(p),$$
$$= \frac{1}{(2\pi)^4}\int d^4k\, d^4p\, e^{i(k+p)\hat{X} - k^\mu p^\nu[\hat{X}_\mu, \hat{X}_\nu]/2}\phi(k)\phi(p), \tag{4}$$

where we used the Baker–Campbell–Hausdorff formula. Thus, the NC version of a field theory is given by replacing field products by the *star product* defined as

$$\hat{\Phi}_1(\hat{X})\hat{\Phi}_2(\hat{X}) \leftrightarrow (\Phi_1 * \Phi_2)(x),$$
$$(\Phi_1 * \Phi_2)(x) = \exp\left[\frac{i}{2}\frac{\partial}{\partial\xi^\mu}\,\theta^{\mu\nu}\frac{\partial}{\partial\eta^\nu}\right]\Phi_1(x+\xi)\Phi_2(x+\eta)\Big|_{\xi=\eta=0}. \tag{5}$$

It obeys the associative law. To the leading order in θ, the star product is given by

$$\Phi_1 * \Phi_2 = \Phi_1\Phi_2 + \frac{i}{2}\theta^{\mu\nu}\partial_\mu\Phi_1\partial_\nu\Phi_2 + \mathrm{O}(\theta^2). \tag{6}$$

It is useful to define a generalized commutator known as the *Moyal bracket* (MB) by the relation

$$[\Phi_1, \Phi_2]_{\mathrm{MB}} = \Phi_1 * \Phi_2 - \Phi_2 * \Phi_1. \tag{7}$$

As one can see, the MB of coordinates,

$$[x_\mu, x_\nu]_{\mathrm{MB}} = x_\mu * x_\nu - x_\nu * x_\mu, \tag{8}$$

[a] e-mail: sceminan@cumhuriyet.edu.tr
[b] e-mail: alexandre.kisselev@ihep.ru (corresponding author)

in agreement with the commutator relation on the NC space-time (1).

There is a relation between the matrix $c_{\mu\nu}$ (2) and the Maxwell field strength, since in string theory the quantization of NC quantum field theory is described by the excitations of D-branes in the presence of the background EM field [6–9]. The c_{0i} coefficients are defined by the direction of a background electric field, $\mathbf{E} = (c_{01}, c_{02}, c_{03})/\Lambda_{\mathrm{NC}}^2$. The c_{ij} elements are related to a background magnetic field, $\mathbf{B} = (c_{23}, c_{02}, -c_{12})/\Lambda_{\mathrm{NC}}^2$.

Note that theories with nonzero c_{0i} in (1) do not generally obey unitarity [15–18]. However, theories with only space-space noncommutativity, $c_{ij} \neq 0$, $c_{0i} = 0$, are unitary.

2 Noncommutative QED

Noncommutative QED (NCQED), based on the group $U(1)$, has been studied in a number of papers [19–28]. It was shown that unbroken $U(N)$ gauge theory is both gauge invariant and renormalizable at the one-loop level [19,23]. The pure noncommutative $U(1)$ Yang-Mills action is defined as

$$S_{\mathrm{NCQED}} = -\frac{1}{4e^2} \int d^4x\, F_{\mu\nu} * F^{\mu\nu}, \tag{9}$$

with

$$F_{\mu\nu} = \partial_\mu A_\nu - \partial_\nu A_\mu - i[A_\mu, A_\nu]_{\mathrm{MB}}. \tag{10}$$

We see that even in the $U(1)$ case the potential A_μ couples to itself. One can easily check that the action (9) is invariant under $U(1)$ transformation defined as

$$A_\mu(x) \to A'_\mu(x) = U(x) * A_\mu(x) * [U(x)]^{-1} + iU(x) * \partial_\mu [U(x)]^{-1}, \tag{11}$$

where

$$U(x) = e^{i\alpha(x)} = 1 + i\alpha(x) - \frac{1}{2}\alpha(x) * \alpha(x) + \cdots . \tag{12}$$

The covariant derivative

$$D_\mu \varphi = \partial_\mu \varphi - iA_\mu * \varphi \tag{13}$$

transforms covariantly. The $*$ product admits only the fields φ with charge 0 or ± 1 [20]. The field strength transforms as

$$F_{\mu\nu} \to F'_{\mu\nu} = U(x) * F_{\mu\nu} * [U(x)]^{-1}. \tag{14}$$

Using relations $U * U^{-1} = U^{-1} * U = I$ and the cyclic property of the star product under the integral [22], we find that

$$S_{\mathrm{NCQED}} = -\frac{1}{4e^2} \int d^4x\, F_{\mu\nu} F^{\mu\nu}. \tag{15}$$

The 2-point photon function is identical in NC and commutative spaces, since the quadratic term in (15) remains the same,

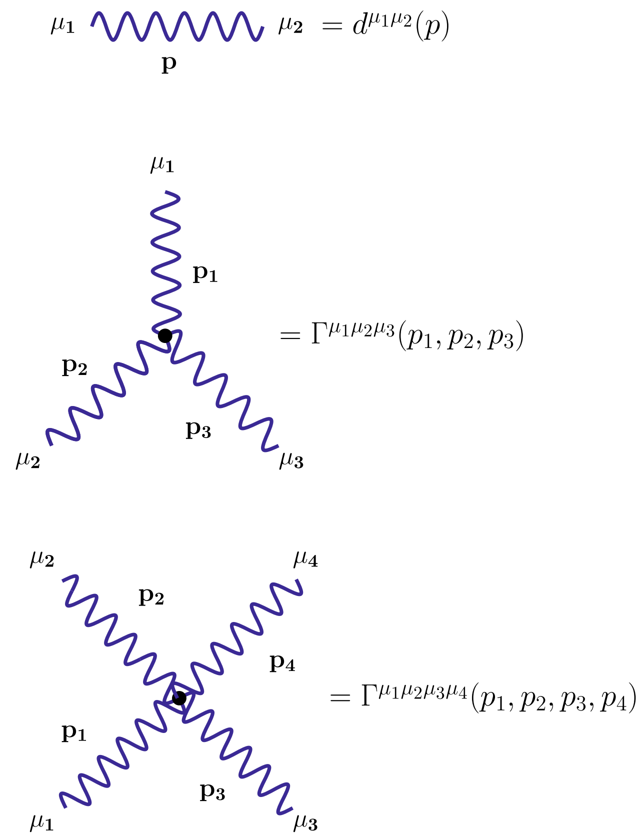

Fig. 1 The Feynman rules of the noncommutative QED

$$d^{\mu_1\mu_2}(p) = -i\frac{g^{\mu_1\mu_2}}{p^2 + i\varepsilon}. \tag{16}$$

Due to the presence of the $*$ product and MB bracket, the theory reveals *non-Abelian* nature. Namely, both 3-point and 4-point photon vertices are generated. The Feynman rules of the pure NCQED [29–32] are shown in Fig. 1.

They are given by the following expressions

$$\begin{aligned}
\Gamma^{\mu_1\mu_2\mu_3}(p_1, p_2, p_3) &= -2e \sin\left(\frac{1}{2} p_1 \wedge p_2\right) \\
&\quad \times \left[(p_1 - p_2)^{\mu_3} g^{\mu_2\mu_3} \right. \\
&\quad + (p_2 - p_3)^{\mu_1} g^{\mu_2\mu_3} \\
&\quad \left. + (p_3 - p_1)^{\mu_2} g^{\mu_3\mu_1}\right], \\
&\Gamma^{\mu_1\mu_2\mu_3\mu_4}(p_1, p_2, p_3, p_4) \\
&= -4ie^2 \Big[\left(g^{\mu_1\mu_3} g^{\mu_2\mu_4} - g^{\mu_1\mu_4} g^{\mu_2\mu_3}\right) \\
&\quad \times \sin\left(\frac{1}{2} p_1 \wedge p_2\right) \sin\left(\frac{1}{2} p_3 \wedge p_4\right) \\
&\quad + \left(g^{\mu_1\mu_4} g^{\mu_2\mu_3} - g^{\mu_1\mu_2} g^{\mu_3\mu_4}\right) \\
&\quad \times \sin\left(\frac{1}{2} p_1 \wedge p_3\right) \sin\left(\frac{1}{2} p_2 \wedge p_4\right) \\
&\quad + \left(g^{\mu_1\mu_2} g^{\mu_3\mu_4} - g^{\mu_1\mu_3} g^{\mu_2\mu_4}\right)
\end{aligned} \tag{17}$$

$$\times \sin\left(\frac{1}{2}\, p_1 \wedge p_4\right)$$
$$\times \sin\left(\frac{1}{2}\, p_2 \wedge p_3\right)\Bigg], \tag{18}$$

where the wedge product is defined as

$$p \wedge k = p^\mu k^\nu \theta_{\mu\nu} = \frac{p^\mu k^\nu c_{\mu\nu}}{\Lambda_{\rm NC}^2}. \tag{19}$$

Note that $p \wedge k = -k \wedge p$ and $p \wedge p = 0$. As one can see, the Feynman rules are very similar to those in *non-abelian* gauge theory, with the structure constants replaced by factors $2\sin[(p_i \wedge p_j)/2]$. These factors arise as a consequence of the MB. Indeed, we have

$$[A_\mu, A_\nu]_{\rm MB} = i \int d^4 p_i\, d^4 p_j\, e^{i(p_i+p_j)x} A_\mu(p_i) A_\nu(p_j) \times \left[2\sin\left(\frac{1}{2}\, p_i \wedge p_j\right)\right]. \tag{20}$$

Thus, NCQED predicts new tree-level contributions to the $\gamma\gamma \to \gamma\gamma$ collision.

Note that $c_{\mu\nu}$ (2) is not a tensor. It means that the Lorentz symmetry is explicitly violated. However, it is quite different from Lorentz breaking models discussed often in the literature, since it can hold only at energies of order $\Lambda_{\rm NC}$. Moreover, since the NCQED is CPT invariant, available experimental bounds on observables which are *simultaneously* CPT and Lorentz violating cannot be used to constrain NCQED.

A number of noncommutative extensions of the Standard Model is constructed [33–41]. Since we are interested in the light-by-light collision, we will work in the framework of the NCQED.

3 Light-by-light scattering at the LHC

The observable signatures in a number of NCQED processes in e^+e^- collisions has been considered in [42–47]. The light-by-light (LBL) scattering in ultraperipheral Pb+Pb collisions in the NCQED context have been recently studied in [48,49]. Our goal is to examine the LBL scattering in pp collisions at the 14 TeV LHC through the process $pp \to p(\gamma\gamma)p \to p'(\gamma\gamma)p'$. Here the final state photons are detected in the central detector and the scattered intact protons are measured with forward detectors.

To detect the protons scattered at small angles, so-called forward detectors are needed. The ATLAS is equipped with the Absolute Luminosity For ATLAS (ALFA) [50,51] and ATLAS Forward Physics (AFP) [52,53]. The CMS collaboration uses the Precision Proton Spectrometer (PPS) as a subdetector which was born from a collaboration between the CMS and TOTEM [54] (previously named CT-PPS). The ALFA system is made of four Roman Pot stations located in a distance of about 240 m at both sides of the ATLAS interaction point. The AFP detector consists of four detectors placed symmetrically with respect to the ATLAS interaction point at 205 m (NEAR stations) and 217 m (FAR stations). The PPS detector has four Roman Pots on each side placed symmetrically in the primary vacuum of the LHC beam pipe, at a distance between 210 and 220 m from the CMS interaction point. These forward detectors are installed as close as a few mm to the beamline to tag the intact protons after elastic photon emission. It allows detecting the fractional proton momentum loss in the interval $\xi_{\rm min} < \xi < \xi_{\rm max}$. The larger value of ξ can be achieved when a detector is installed closer to the interaction point.

Two types of examinations included by the AFP are (i) exploratory physics (anomalous couplings between γ and Z or W bosons, exclusive production, etc.); (ii) standard QCD physics (double Pomeron exchange, exclusive production in the jet channel, single diffraction, $\gamma\gamma$ physics, etc.). PPS experiments aim at a study of the elastic proton–proton interactions, the proton–proton total cross-section and other diffractive processes. Moreover, precise search can be done with the forward detectors [55–57]. In such interactions involving high energy and high luminosity, the pile-up background may be formed. This background can be extremely reduced by using kinematics, timing constraints, and exclusivity conditions [58–60]. There are many phenomenological papers that use photon-induced reactions for searching new physics at the LHC [61–82].

We examine the process $pp \to p\gamma\gamma p \to p'(\gamma\gamma)p'$. Emitted photons have very small virtualities, hence they are almost-real photons and can be considered as on-mass-shell particles. The main detector (ATLAS or CMS) registers the final state $\gamma\gamma$, while the proton momentum loss ξ is measured by the forward detector (AFP or CT-PPS). This makes it possible to determine the invariant energy of the $\gamma\gamma$ collision, $W = 2E\sqrt{\xi_1\xi_2}$, where E is the energy of the incoming protons. These type of collision can be studied using equivalent photon approximation (EPA) [83–85]. In the EPA, a photon emitted with small angles by the protons shows the following spectrum in photon virtuality Q^2 and energy fraction $x = E_\gamma/E$,

$$f(x,Q^2) = \frac{\alpha}{\pi}\frac{1}{xQ^2}\left[(1-x)\left(1-\frac{Q^2_{\rm min}}{Q^2}\right)F_E(Q^2) + \frac{x^2}{2}F_M(Q^2)\right], \tag{21}$$

where

$$Q^2_{\rm min} = \frac{m_p^2 x^2}{1-x}, \quad F_E = \frac{4m_p^2 G_E^2 + Q^2 G_M^2}{4m_p^2 + Q^2}, \quad F_M = G_M^2, \tag{22}$$

$$G_E^2 = \frac{G_M^2}{\mu_p^2} = \left(1 + \frac{Q^2}{Q_0^2}\right)^{-4}, \quad Q_0^2 = 0.71,$$
$$\mu_p^2 = 7.78 \text{ GeV}^2. \tag{23}$$

Here, m_p is the mass of the proton, μ_p is its magnetic moment, F_E and F_M are electric and magnetic form factors of the proton. To obtain the cross section of the process $pp \to p(\gamma\gamma)p \to p'(\gamma\gamma)p'$, the cross section $d\sigma_{\gamma\gamma\to\gamma\gamma}$ of the subprocess $\gamma\gamma \to \gamma\gamma$ should be integrated over the photon spectrum,

$$d\sigma = \int dW \, \frac{dL_{\gamma\gamma}}{dW} \, d\sigma_{\gamma\gamma\to\gamma\gamma}(W). \tag{24}$$

The effective photon luminosity in (24) is given by

$$\frac{dL_{\gamma\gamma}}{dW} = \frac{W}{2E^2} \int_{Q_{\min}^2}^{Q_{max}^2} dQ_1^2 \int_{Q_{\min}^2}^{Q_{\max}^2} dQ_2^2 \int_{x_{\min}}^{x_{\max}} \frac{dx}{x} \times f_1\left(\frac{W^2}{4E^2x}, Q_1^2\right) f_2(x, Q_2^2), \tag{25}$$

where

$$x_{\min} = \max(\xi_{\min}, W^2/(4E^2\xi_{\max})), \quad x_{\max} = \xi_{\max}. \tag{26}$$

We put $Q_{\max}^2 = 2$ GeV^2, since the contribution of more than this value is very small.

The diagrams describing the $\gamma\gamma \to \gamma\gamma$ scattering in the order e^2 are presented in Fig. 2. The nonzero independent helicity amplitudes of NCQED have been derived in [44,49]

$$\begin{aligned}
&M^{\rm NC}_{++++}(p_1, p_2; k_1, k_2) \\
&= -32\pi\alpha\left[\frac{s}{t}\sin\left(\frac{1}{2}p_1\wedge k_1\right)\sin\left(\frac{1}{2}p_2\wedge k_2\right) + \frac{s}{u}\sin\left(\frac{1}{2}p_1\wedge k_2\right)\sin\left(\frac{1}{2}p_2\wedge k_1\right)\right], \\
&M^{\rm NC}_{+--+}(p_1, p_2; k_1, k_2) \\
&= -32\pi\alpha\left[\frac{t}{s}\sin\left(\frac{1}{2}p_1\wedge k_1\right)\sin\left(\frac{1}{2}p_2\wedge k_2\right) + \frac{t^2}{su}\sin\left(\frac{1}{2}p_1\wedge k_2\right)\sin\left(\frac{1}{2}p_2\wedge k_1\right)\right],
\end{aligned} \tag{27}$$

where $\alpha = e^2/(4\pi)$, and $s = (p_1 + p_2)^2$, $t = (p_1 - k_1)^2$, $u = (p_1 - k_2)^2$ are Mandelstam variables of the $\gamma\gamma \to \gamma\gamma$ process ($s + t + u = 0$). To derive expressions (27) form those presented in [44], we have used the Moyal-Weyl star product Jacobi identity in momentum space [49]

$$\sin\left(\frac{1}{2}p_1\wedge p_2\right)\sin\left(\frac{1}{2}k_1\wedge k_2\right) + \sin\left(\frac{1}{2}p_1\wedge k_2\right)\sin\left(\frac{1}{2}p_2\wedge k_1\right) - \sin\left(\frac{1}{2}p_1\wedge k_1\right)\sin\left(\frac{1}{2}p_2\wedge k_2\right) = 0. \tag{28}$$

The amplitude $M^{\rm NC}_{++-+-}$ is defined by the crossing relation

$$\begin{aligned}
&M^{\rm NC}_{+-+-}(p_1, p_2; k_1, k_2) = M_{+--+}(p_1, p_2; k_2, k_1) \\
&= -32\pi\alpha\left[\frac{u^2}{st}\sin\left(\frac{1}{2}p_1\wedge k_1\right)\sin\left(\frac{1}{2}p_2\wedge k_2\right) + \frac{u}{s}\sin\left(\frac{1}{2}p_1\wedge k_2\right)\sin\left(\frac{1}{2}p_2\wedge k_1\right)\right].
\end{aligned} \tag{29}$$

The other nonzero NC helicity amplitudes are related to the amplitudes (27) and (29) by the parity relations

$$\begin{aligned}
M^{\rm NC}_{----}(p_1, p_2; k_1, k_2) &= M^{\rm NC}_{++++}(p_1, p_2; k_1, k_2), \\
M^{\rm NC}_{-++-}(p_1, p_2; k_1, k_2) &= M^{\rm NC}_{+--+}(p_1, p_2; k_1, k_2), \\
M^{\rm NC}_{-+-+}(p_1, p_2; k_1, k_2) &= M^{\rm NC}_{+-+-}(p_1, p_2; k_1, k_2).
\end{aligned} \tag{30}$$

After simple arithmetic we find from (27), (29), and (30)

$$\begin{aligned}
\sum_{\rm pol}|M_{\rm NC}|^2 &= 2\left(|M^{\rm NC}_{++++}|^2 + |M^{\rm NC}_{+--+}|^2 + |M^{\rm NC}_{+-+-}|^2\right) \\
&= 2(32\pi\alpha)^2\,\frac{s^4+t^4+u^4}{s^2}\left[\frac{1}{t}\sin\left(\frac{1}{2}p_1\wedge k_1\right)\sin\left(\frac{1}{2}p_2\wedge k_2\right) + \frac{1}{u}\sin\left(\frac{1}{2}p_1\wedge k_2\right)\sin\left(\frac{1}{2}p_2\wedge k_1\right)\right]^2.
\end{aligned} \tag{31}$$

As it is shown in Appendix A, this equation can be written as

$$\begin{aligned}
\sum_{\rm pol}|M_{\rm NC}|^2 &= 2\left(|M^{\rm NC}_{++++}|^2 + |M^{\rm NC}_{+--+}|^2 + |M^{\rm NC}_{+-+-}|^2\right) \\
&= 2(-2)(32\pi\alpha)^2 \\
&\quad\times\left\{\left(\frac{s}{u}+\frac{u}{s}+\frac{su}{t^2}\right)\left[\sin\left(\frac{1}{2}p_1\wedge k_1\right)\sin\left(\frac{1}{2}p_2\wedge k_2\right)\right]^2\right. \\
&\quad+\left(\frac{t}{s}+\frac{s}{t}+\frac{st}{u^2}\right)\left[\sin\left(\frac{1}{2}p_1\wedge k_2\right)\sin\left(\frac{1}{2}p_2\wedge k_1\right)\right]^2 \\
&\quad\left.+\left(\frac{u}{t}+\frac{t}{u}+\frac{tu}{s^2}\right)\left[\sin\left(\frac{1}{2}p_1\wedge p_2\right)\sin\left(\frac{1}{2}k_1\wedge k_2\right)\right]^2\right\},
\end{aligned} \tag{32}$$

in a full agreement with eq. (93) in [49], after changing momenta notations, $(p_1, p_2, k_1, k_2) \to (k_1, k_2, k_4, k_3)$. Note that the second term in the brackets in Eq. (32) is obtained from the first term if one uses the replacements $k_1 \rightleftarrows k_2$, $t \rightleftarrows u$. Analogously, the third term comes from the first one after the replacements $k_1 \rightleftarrows p_2$, $t \rightleftarrows s$.

There is a one-to one correspondence between the color ordering in QCD and the star product in pure NCQED [86]. As it was mentioned in the end of Sect. 2, all vertices of NCQED are similar to gluon vertices in QCD in which the structure constants $f^{a_i a_j c}$ are replaced by $2\sin[(l_i \wedge l_j)/2]$. A correspondence between NCQED and QCD amplitudes can be achieved, if one makes in (32) the following replacements [49]

$$\left[2\sin\left(\frac{1}{2}l_i \wedge l_j\right)\right]^2 \left[2\left(\frac{1}{2}l_k \wedge l_r\right)\right]^2 \\ \rightarrow \left(f^{a_i a_j c} f^{a_i a_j d}\right)\left(f^{a_k a_r c} f^{a_k a_r d}\right) = 3^2\delta^{cd}\delta^{cd} = 72, \tag{33}$$

where (l_i, l_j, l_k, l_r) is a combination of the photon momenta p_1, p_2, k_1, k_2, and the sum over all color indices is assumed. The gluon–gluon amplitude square is a sum of helicity amplitudes square,

$$|M_{gg\to gg}|^2 = \frac{1}{8^2 2^2}\sum_{\text{pol}} |M_{\lambda_1\lambda_2\lambda_3\lambda_4}|^2, \tag{34}$$

and the differential cross section is given by

$$\frac{d\sigma}{d\Omega}(gg \to gg) = \frac{1}{64\pi^2}\frac{|M_{gg\to gg}|^2}{s}. \tag{35}$$

After summation over Mandelstam variables in (32),

$$\left(\frac{s}{u} + \frac{u}{s} + \frac{su}{t^2}\right) + \left(\frac{t}{s} + \frac{s}{t} + \frac{st}{u^2}\right) + \left(\frac{u}{t} + \frac{t}{u} + \frac{tu}{s^2}\right) \\ = -\left(3 - \frac{tu}{s^2} - \frac{su}{t^2} - \frac{ts}{u^2}\right), \tag{36}$$

and replacement $\alpha \to \alpha_s$, we come from (32)–(35) to the well-known expression for the differential cross section of the gluon–gluon scattering [87]

$$\frac{d\sigma}{d\Omega}(gg \to gg) = \frac{9\alpha_s^2}{8s}\left(3 - \frac{tu}{s^2} - \frac{su}{t^2} - \frac{ts}{u^2}\right). \tag{37}$$

Thus, our NC amplitude square and its counterpart in QCD are closely connected.

4 Numerical analysis

We work in the c.m.s. of the colliding protons. Let x_1 and x_2 be momentum fractions of the protons carried by the scattered photons which can be considered to be on-shell particles. Then the photon momenta look like

$$p_1 = x_1 E(1, 0, 0, 1), \quad p_2 = x_2 E(1, 0, 0, -1). \tag{38}$$

Thus, the $\gamma(p_1) + \gamma(p_2) \to \gamma(k_1) + \gamma(k_2)$ collision goes in the *non-center-of mass* system. For the massless case the momenta of the outgoing photons are given by

$$k_1 = E_1(1, s_\theta c_\phi, s_\theta s_\phi, c_\theta), \\ k_2 = \big((x_1 + x_2)E - E_1, -E_1 s_\theta c_\phi, \\ -E_1 s_\theta s_\phi, (x_1 - x_2)E - E_1 c_\theta\big), \tag{39}$$

where

$$E_1 = \frac{2x_1 x_2 E}{x_1 + x_2 - (x_1 - x_2)c_\theta}. \tag{40}$$

Here $c_\theta = \cos\theta$, $s_\theta = \sin\theta$, $c_\phi = \cos\phi$, $s_\phi = \sin\phi$, with θ and ϕ being the scattering angles of the outgoing photon with momentum k_1.

Then the wedge products of the photon momenta in the formulas for the NC helicity amplitudes take the form [44,49]

$$p_1 \wedge k_1 = -\frac{x_1 E_1 E}{\Lambda_{\text{NC}}^2}[c_{03}(1 - c_\theta) - (c_{01} - c_{13})s_\theta c_\phi \\ - (c_{02} - c_{23})s_\theta s_\phi], \\ p_2 \wedge k_1 = \frac{x_2 E_1 E}{\Lambda_{\text{NC}}^2}[c_{03}(1 + c_\theta) + (c_{01} + c_{13})s_\theta c_\phi \\ + (c_{02} + c_{23})s_\theta s_\phi], \\ p_1 \wedge k_2 = -\frac{x_1 E_1 E}{\Lambda_{\text{NC}}^2}\left[\frac{x_2}{x_1}(1 + c_\theta) + (c_{01} - c_{13})s_\theta c_\phi \\ + (c_{02} - c_{23})s_\theta s_\phi\right], \\ p_2 \wedge k_2 = \frac{x_2 E_1 E}{\Lambda_{\text{NC}}^2}\left[\frac{x_1}{x_2}(1 - c_\theta) - (c_{01} + c_{13})s_\theta c_\phi \\ - (c_{02} + c_{23})s_\theta s_\phi\right]. \tag{41}$$

The Mandelstam variables of the $\gamma\gamma \to \gamma\gamma$ process are given by

$$s = 4E^2 x_1 x_2, \quad t = -2x_1 E E_1(1 - c_\theta), \\ u = -2x_2 E E_1(1 + c_\theta)]. \tag{42}$$

The differential cross section of the $\gamma\gamma \to \gamma\gamma$ process in the frame (38)–(39) is given by [49]

$$\frac{d\sigma}{d\Omega}(\gamma\gamma \to \gamma\gamma) = \left(\frac{E_1}{4\pi s}\right)^2 \frac{1}{2^2}\sum_{\text{pol}} |M^{\text{NC}}_{\lambda_1\lambda_2\lambda_3\lambda_4} \\ + M^{\text{SM}}_{\lambda_1\lambda_2\lambda_3\lambda_4}|^2, \tag{43}$$

where $d\Omega = \sin\theta d\theta d\phi$. Note that the first factor in the right-hand side of this equation coincides with the conventional factor $1/(64\pi^2 s)$ only if $x_1 = x_2$.

To do our calculations, we choose the region of $0.015 < \xi < 0.15$ for both protons which is a standard acceptance in the central detectors at the nominal accelerator and beam conditions. It is in accordance with the intervals for ξ used by the ATLAS [88] and CMS-TOTEM [89] collaborations, as well as in several papers that examine processes with the proton tagging at the LHC [90–96]. We also have applied the cut on the rapidity of the outgoing photons, $|\eta| < 2.5$, in all calculations.

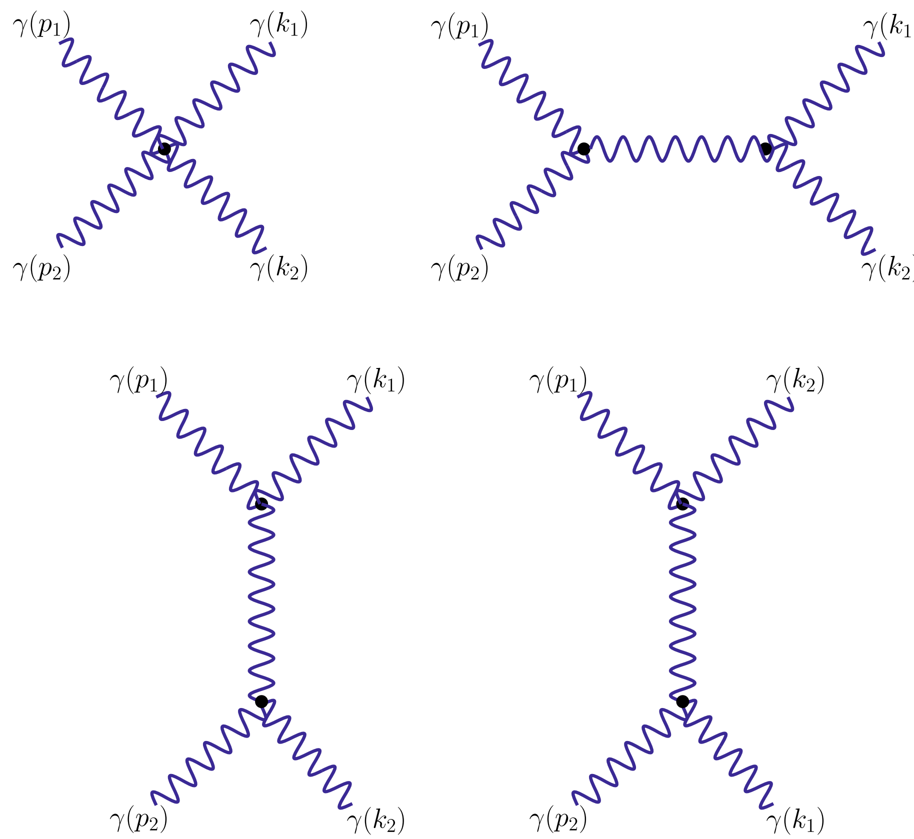

Fig. 2 The tree level contributions to the $\gamma\gamma \to \gamma\gamma$ scattering in the noncommutative QED

The SM contribution to the $\gamma\gamma \to \gamma\gamma$ scattering is described by diagrams with charged fermion loops and W boson loops [97–101]. As it is shown in [73], the gluon-initiated production of two photons via quark loops can be neglected for the center-of-mass energy greater than 200 GeV. In our study, minimum mass energy may be $2 \times 7000\,\text{GeV} \times 0.015 = 210\,\text{GeV}$ due to $\xi_{\text{min}} = 0.015$ value. Therefore, we could safely ignore QCD corrections. Explicit analytical expressions for the SM helicity amplitudes, both for the fermion and W boson terms are too long. That is why we do not present them here. They can be found in [102]. In such high-energy and luminosity collisions, pile-up backgrounds can occur. With the use of kinematics, exclusivity conditions, and timing constraints such backgrounds can be extremely reduced [58,59].

As it follows from Eqs. (27), (29), (30), and (41), two options, $c_{01} = 1$, with all other $c_{\mu\nu}$ vanishing, and $c_{13} = 1$, with all other $c_{\mu\nu}$ vanishing, result in the same NC helicity amplitudes. The same is true for the amplitudes with $c_{02} = 1$ and $c_{23} = 1$. Given only one of the parameters $c_{\mu\nu}$ is taken to be nonzero, the NC amplitudes are insensitive to its sign, since they are invariant under the $c_{\mu\nu} \to -c_{\mu\nu}$ replacement. Note also that four-photon NC helicity amplitudes do not depend on c_{12}. Thus, only three possibilities should be addressed: (i) $c_{03} = 1$, with all other $c_{\mu\nu}$ vanishing; (ii) $c_{13} = 1$, all other NC parameters are zero; (iii) $c_{23} = 1$, with all other $c_{\mu\nu}$ vanishing.

In Fig. 3 we show the results of our calculations of the total and SM differential cross section for the diphoton production at the 14 TeV LHC with intact protons. The cross section is presented as a function of the invariant mass of outgoing photons, $m_{\gamma\gamma}$, for two values of the NC scale Λ_{NC}. We see that in the region $m_{\gamma\gamma} > 400(600)$ GeV the NC contribution strongly dominate the SM one for $\Lambda_{\text{NC}} = 0.5(1.0)$ TeV. For both values of the NC scale, the time-space NC (blue curves in Fig. 3) is larger that the space-space NC (red curves). Only for $\Lambda_{\text{NC}} = 0.5$ TeV and $m_{\gamma\gamma} > 1800$ GeV the time-space and space-space curves merge. From Eqs. (27), (29), and (41) one makes sure that after integrations over angular variables, the NC amplitudes should give the same contribution to the differential cross section both for $c_{13} = 1$ and for $c_{23} = 1$. Our numerical calculations confirm this statement. That is why, we do not present curves for case (iii) in Fig. 3.

In Fig. 4 the total and SM cross sections $\sigma(m_{\gamma\gamma} > m_{\gamma\gamma,\,\text{min}})$ versus $m_{\gamma\gamma,\,\text{min}}$, the minimal invariant mass of the outgoing photons, is presented. As one can see, for $\Lambda_{\text{NC}} = 0.5$ TeV this cross section is approximately two order of magnitude larger than the SM cross section in all mass region. For $\Lambda_{\text{NC}} = 1$ TeV the deviation of the cross section from the SM one is also very large and becomes more and more prominent as $m_{\gamma\gamma,\,\text{min}}$ grows. Thus, the bigger is the value of $m_{\gamma\gamma,\,\text{min}}$, the larger is the difference between the new physics and SM. Note that the time-space NC exceeds the space-space NC for all $m_{\gamma\gamma,\,\text{min}}$. Only for $\Lambda_{\text{NC}} = 0.5$

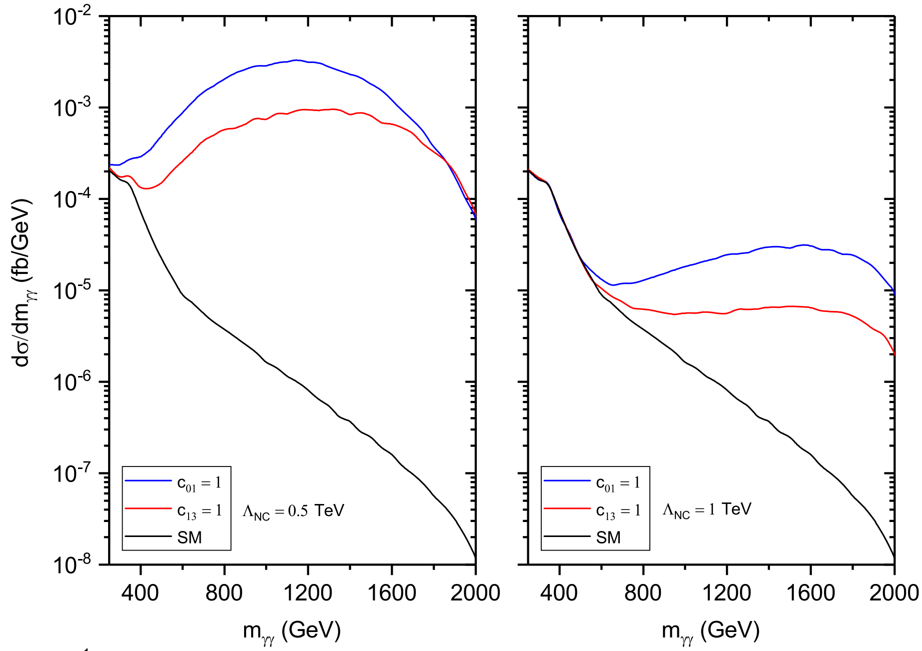

Fig. 3 The differential cross section for the $pp \to p\gamma\gamma p \to p'\gamma\gamma p'$ scattering at the LHC in the noncommutative QED versus invariant mass of the final photons

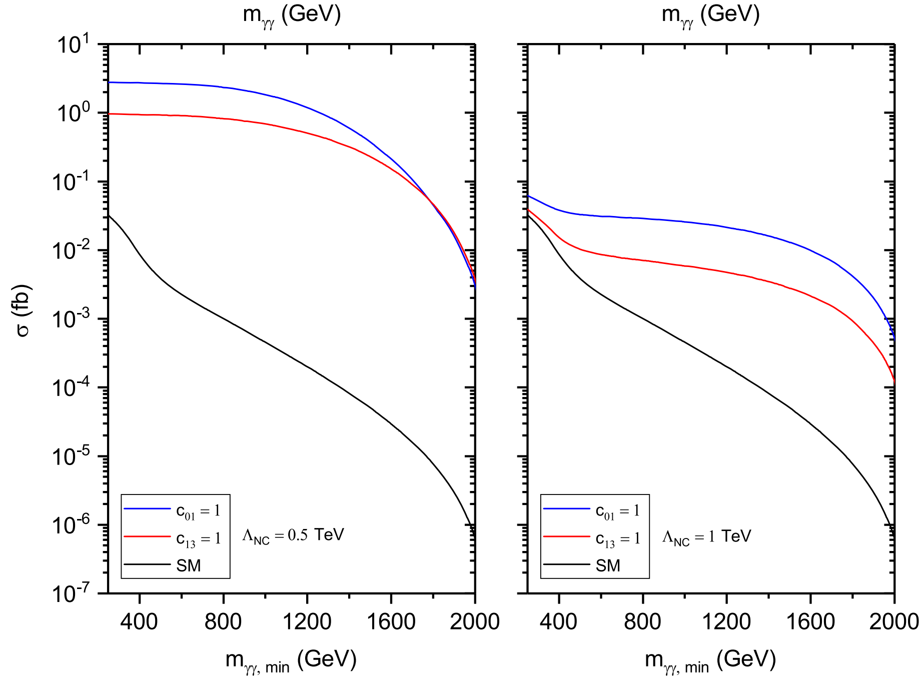

Fig. 4 The cross section $\sigma(m_{\gamma\gamma} > m_{\gamma\gamma,\,\min})$ for the $pp \to p\gamma\gamma p \to p'\gamma\gamma p'$ scattering at the LHC in the noncommutative QED versus minimal invariant mass of the diphoton system

TeV it becomes comparable with the space-space NC in the large $m_{\gamma\gamma,\,\min}$ region.

Knowing cross sections and SM backgrounds, we have calculated upper bounds on the NC scale $\Lambda_{\rm NC}$ which can be obtained from the $pp \to p\gamma\gamma p \to p'\gamma\gamma p'$ scattering at the LHC. To obtain the exclusion region, we applied the following equation for the statistical significance (SS) [103]

$$SS = \sqrt{2[(S - B\ \ln(1 + S/B)]}, \qquad (44)$$

where S is the number of signal events and B is the number of background events. We define the regions $SS \leqslant 1.645$ as the regions that can be excluded at the 95% CL. To reduce the SM background, we used the cut $m_{\gamma\gamma} > 1000$ GeV. The results are shown in Fig. 5. We see that two-photon process at the LHC can probe the NC scale $\Lambda_{\rm NC}$ up to 1.64(1.35) TeV for time-space (space-space) NC parameters for the integrated luminosity $L = 3000$ fb^{-1}. If $L = 1000$ fb^{-1}, the upper bounds are approximately 1.40 TeV and 1.15 TeV, for time-space and space-space NC parameters, respectively.

5 Conclusions

We have examined the light-by-light scattering in the non-commutative (NC) quantum electrodynamics (NCQED) in the $pp \to p\gamma\gamma p \to p'\gamma\gamma p'$ collision at the 14 TeV LHC.

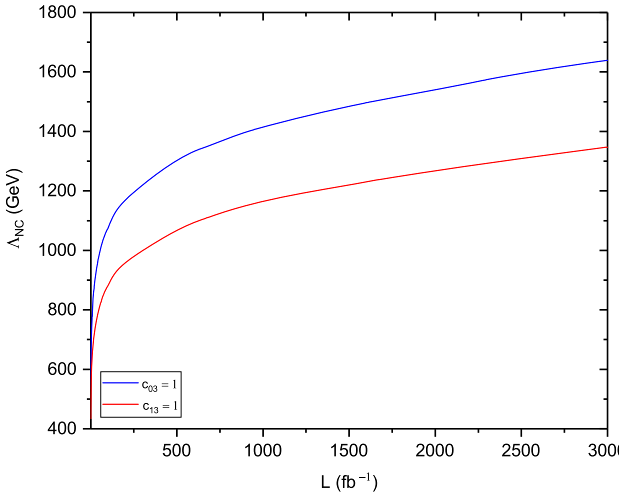

Fig. 5 95% CL bounds on the noncommutative scale Λ_{NC} coming from the $pp \to p\gamma\gamma p \to p'\gamma\gamma p'$ scattering as functions of integrated luminosity of proton–proton collision at 14 TeV. The curves are obtained with the use of the cut on diphoton invariant mass, $m_{\gamma\gamma} > 1000$ GeV

The NC geometry of space-time appears within a framework of string theory. NCQED is based on the $U(1)$ group, but it exhibits the non-Abelian nature in having both 3-photon and 4-photon vertices in the Lagrangian. That is why the $\gamma\gamma \to \gamma\gamma$ scattering must be sensitive to the NC contributions at the tree level, see Fig. 2.

We have calculated the differential cross sections as functions of the invariant mass of the outgoing photons (Fig. 3), as well as the cross sections as functions of the minimum invariant mass of the outgoing photons (Fig. 4). Both time-space and space-space NC parameters have been considered. The SM background is defined by the contributions from the W and charged fermion loops. It allowed us to estimate the 95% CL bounds for the NC scale Λ_{NC}. We have shown that the scales up to $\Lambda_{NC} = 1.64(1.35)$ TeV can be probed at the LHC, for the time-space (space-space) NC parameters, see Fig. 5. Our bounds are stronger than the limits that can be obtained in the 4-photon scattering at high energy linear colliders [44]. Note that $\gamma\gamma \to \gamma\gamma$ is the more appropriate channel to probe Λ_{NC} also in Pb-Pb collisions at the LHC [49].

In the present paper we have made tree level calculations. The one-loop corrections in NC Yang-Mills theories were considered in a number of papers [19,20,29,104–106]. In particular, one-loop beta function in NC QED has been calculated [19,20]. In contrast to the commutative theory, it was shown that NC QED is asymptotically free (provided the number of copies of electron fields is less than six) [19,20]. Note that the very value of the beta function is independent of the NC parameter $\theta_{\mu\nu}$. Since the coupling constant decreases as energy scale grows, we expect that an impact of loop corrections to our tree level calculations should be small.

Acknowledgements We would like to thank Josip Trampetić for discussions and sending us the file with the outcome of calculations of noncommutative helicity amplitudes.

Data Availability Statement This manuscript has no associated data or the data will not be deposited. [Authors' comment: We didn't use experimental data in our calculations.]

Funded by SCOAP^3. SCOAP^3 supports the goals of the International Year of Basic Sciences for Sustainable Development.

Appendix A

The right-hand side of Eq. (31), with the factor $2(32\pi\alpha)^2$ omitted, looks like

$$I = \frac{s^4+t^4+u^4}{s^2}\left[\frac{1}{t}\sin\left(\frac{1}{2}p_1\wedge k_1\right)\sin\left(\frac{1}{2}p_2\wedge k_2\right) + \frac{1}{u}\sin\left(\frac{1}{2}p_1\wedge k_2\right)\sin\left(\frac{1}{2}p_2\wedge k_1\right)\right]^2. \tag{A.1}$$

From the Jacobi identity (28) it follows that

$$\begin{aligned} &2\left[\sin\left(\frac{1}{2}p_1\wedge k_1\right)\sin\left(\frac{1}{2}p_2\wedge k_2\right)\right] \\ &\quad\times\left[\sin\left(\frac{1}{2}p_1\wedge k_2\right)\sin\left(\frac{1}{2}p_2\wedge k_1\right)\right] \\ &\quad=\left[\sin\left(\frac{1}{2}p_1\wedge k_1\right)\sin\left(\frac{1}{2}p_2\wedge k_2\right)\right]^2 \\ &\quad+\left[\sin\left(\frac{1}{2}p_1\wedge k_2\right)\sin\left(\frac{1}{2}p_2\wedge k_1\right)\right]^2 \\ &\quad-\left[\sin\left(\frac{1}{2}p_1\wedge p_2\right)\sin\left(\frac{1}{2}k_1\wedge k_2\right)\right]^2. \end{aligned} \tag{A.2}$$

Then we obtain from (A.1)

$$\begin{aligned} I = -\frac{s^4+t^4+u^4}{stu}\Bigg\{&\frac{1}{t}\left[\sin\left(\frac{1}{2}p_1\wedge k_1\right)\sin\left(\frac{1}{2}p_2\wedge k_2\right)\right]^2 \\ &+\frac{1}{u}\left[\sin\left(\frac{1}{2}p_1\wedge k_2\right)\sin\left(\frac{1}{2}p_2\wedge k_1\right)\right]^2 \end{aligned}$$

$$+\frac{1}{s}\left[\sin\left(\frac{1}{2}p_1\wedge p_2\right)\sin\left(\frac{1}{2}k_1\wedge k_2\right)\right]^2\Bigg\}. \tag{A.3}$$

Using relation $s^4+t^4+u^4=2(s^2t^2+t^2u^2+u^2s^2)$, we get the equation

$$I=(-2)\Bigg\{\left(\frac{s}{u}+\frac{u}{s}+\frac{su}{t^2}\right)\left[\sin\left(\frac{1}{2}p_1\wedge k_1\right)\sin\left(\frac{1}{2}p_2\wedge k_2\right)\right]^2 +\left(\frac{t}{s}+\frac{s}{t}+\frac{st}{u^2}\right)\left[\sin\left(\frac{1}{2}p_1\wedge k_2\right)\sin\left(\frac{1}{2}p_2\wedge k_1\right)\right]^2 +\left(\frac{u}{t}+\frac{t}{u}+\frac{tu}{s^2}\right)\left[\sin\left(\frac{1}{2}p_1\wedge p_2\right)\sin\left(\frac{1}{2}k_1\wedge k_2\right)\right]^2\Bigg\}, \tag{A.4}$$

that results in formula (32).

References

1. H.S. Snyder, Quantized space-time. Phys. Rev. **71**, 38 (1947)
2. H.S. Snyder, The electromagnetic field in quantized spacetime. Phys. Rev. **72**, 68 (1947)
3. G. Landi, *An Introduction to Noncommutative Spaces and Their Geometries*. Lecture Notes in Physics. New Series m: Monographs, vol. 51 (Springer, Berlin, 1997). arXiv:hep-th/9701078
4. M.R. Douglas, N.A. Nekrasov, Noncommutative field theory. Rev. Mod. Phys. **73**, 977 (2001). arXiv:hep-th/0106048
5. R.J. Szabo, Quantum field theory on noncommutative spaces. Phys. Rep. **378**, 207 (2003). arXiv:hep-th/0109162
6. A. Connes, *Non-commutative Geometry* (Academic Press, New York, 1994)
7. N. Seiberg, E. Witten, String theory and noncommutative geometry. JHEP **09**, 032 (1999). arXiv:hep-th/9908142
8. J. Gomis, M. Kleban, T. Mehen, M. Rangamani, S. Shenker, Noncommutative gauge dynamics from the string worldsheet. JHEP **08**, 011 (2000). arXiv:hep-th/0003215
9. E.T. Akhmedov, P. DeBoer, G.W. Semenoff, Running couplings and triviality of field theories on noncommutative spaces. Phys. Rev. D **64**, 065005 (2001). arXiv:hep-th/0010003
10. H. Weyl, Quantenmechanik und Gruppentheorie. Z. Physik **46**, 1 (1927)
11. H. Weyl, *The Theory of Groups and Quantum Mechanics*, Dover, New York (1931), Translated from Gruppentheorie und Quantenmechanik (Hirzel Verlag, Leipzig, 1928)
12. J.E. Moyal, Quantum mechanics as a statistical theory. Proc. Camb. Philos. Soc. **45**, 99 (1949)
13. J. Madore, S. Schram, P. Schupp, J. Wess, Gauge theory on noncommutative spaces. Eur. Phys. J. C **16**, 161 (2000). arXiv:hep-th/0001203
14. L. Alvarez-Gaume, S.R. Wadia, Gauge theory on a quantum phase space. Phys. Lett. B **501**, 319 (2001). arXiv:hep-th/0006219
15. J. Gomis, T. Mehen, Space-time noncommutative field theories and unitarity. Nucl. Phys. B **591**, 265 (2000). arXiv:hep-th/0005129
16. O. Aharony, J. Gomis, T. Mehen, On theories with light-like noncommutativity. JHEP **09**, 023 (2000). arXiv:hep-th/0006236
17. M. Chaichian, A. Demichev, P. Presnajder, Quantum field theory on noncommutative space-times and the persistence of ultraviolet divergences. Nucl. Phys. B **567**, 360 (2000). arXiv:hep-th/9812180
18. M. Chaichian, A. Demichev, P. Presnajder, A. Tureanu, Space-time noncommutativity, discreteness of time and unitarity. Eur. Phys. J. C **20**, 767 (2001). arXiv:hep-th/0007156
19. C.P. Martin, D. Sanchez-Ruiz, The one-loop UV divergent structure of $U(1)$ Yang–Mills theory on noncommutative R^4. Phys. Rev. Lett. **83**, 476 (1999). arXiv:hep-th/9903077
20. M. Hayakawa, Perturbative analysis on infrared aspects of noncommutative QED on R^4. Phys. Lett. B **478**, 394 (2000). arXiv:hep-th/9912094
21. J.M. Gracia-Bondia, C.P. Martin, Chiral gauge anomalies on noncommutative R^4. Phys. Lett. B **479**, 321 (2000). arXiv:hep-th/0002171
22. I.F. Riad, M.M. Sheikh-Jabbari, Noncommutative QED and anomalous dipole moments. JHEP **08**, 045 (2000). arXiv:hep-th/0008132
23. L. Bonora, M. Salizzon, Renormalization of non-commutative $U(N)$ gauge theories. Phys. Lett. B **504**, 80 (2001). arXiv:hep-th/0011088
24. F. Ardalan, N. Sadooghi, Axial anomaly in noncommutative QED on R^4. Int. J. Mod. Phys. A **16**, 3152 (2001). arXiv:hep-th/0002143
25. F. Ardalan, N. Sadooghi, Anomaly and nonplanar diagrams in noncommutative gauge theories. Int. J. Mod. Phys. A **17**, 123 (2002). arXiv:hep-th/0009233
26. T. Mariz, C.A.S. de Pires, R.F. Ribeiro, Ward identity in noncommutative QED. Int. J. Mod. Phys. **18**, 5433 (2003). arXiv:hep-ph/0211416
27. F. Canfora, M. Kurkov, L. Rosa, P. Vitale, The Gribov problem in noncommutative QED. JHEP **01**, 014 (2016). arXiv:1505.06342
28. K. Morita, Lorentz-invariant non-commutative QED. Prog. Theor. Phys. **108**, 1099 (2002). arXiv:hep-th/0209234
29. A. Armoni, Comments on perturbative dynamics of noncommutative Yang–Mills theory. Nucl. Phys. B **593**, 229 (2001). arXiv:hep-th/0005208
30. M.M. Sheikh-Jabbari, Renormalizability of the supersymmetric Yang–Mills theories on the noncommutative torus. JHEP **06**, 015 (1999). arXiv:hep-th/9903107
31. T. Krajewski, R. Wulkenhaar, Perturbative quantum gauge fields on the noncommutative torus. Int. J. Mod. Phys. A **15**, 1011 (2000). arXiv:hep-th/9903187
32. I. Ya. Aref'eva, D.M. Belov, A.S. Koshelev, O.A. Rytchkov, UV/IR mixing for noncommutative complex scalar field theory, II (interaction with gauge fields). Nucl. Phys. Proc. Suppl. **102**, 11 (2001). arXiv:hep-th/0003176
33. F. Lizzi, G. Mangano, G. Miele, G. Sparano, Fermion Hilbert space and fermion doubling in the noncommutative geometry approach to gauge theories. Phys. Rev. D Phys. Rev. D **55**, 6357 (1997). arXiv:hep-th/9610035
34. J.M. Gracia-Bondia, B. Iochum, T. Schucker, The standard model in noncommutative geometry and fermion doubling. Phys. Lett. B **414**, 123 (1998). arXiv:hep-th/9709145
35. M. Chaichian, P. Prešnajder, M.M. Sheikh-Jabbari, A. Tureaunu, Noncommutative Standard Model: model building. Eur. Phys. J. C **29**, 413 (2001). arXiv:hep-th/0107055
36. X. Calmet, B. Jurco, P. Schupp, J. Wess, M. Wohlgenannt, The Standard model on non-commutative space-time. Eur. Phys. J. C **23**, 363 (2002). arXiv:hep-ph/0111115
37. B. Melic, K. Passek-Kumericki, J. Trampetic, P. Schupp, M. Wohlgenannt, The standard model on non-commutative space-time: electroweak currents and Higgs sector. Eur. Phys. J. C **42**, 483 (2005). arXiv:hep-ph/0502249
38. S. Marculescu, Non-commutative extensions of the standard model. arXiv:hep-th/0508018
39. A. Alboteanu, T. Ohl, R. Ruckl, Noncommutative standard model at $O(\theta^2)$. Phys. Rev. D **76**, 105018 (2007). arXiv:0707.3595

40. F. Besnard, Extensions of the noncommutative Standard Model and the weak order one condition. arXiv:2011.02708
41. F. Besnard, A $U(1)_{B-L}$-extension of the standard model from noncommutative geometry. J. Math. Phys. **62**, 012301 (2021). arXiv:1911.01100
42. P. Mathews, Compton scattering in noncommutative space-time at the next linear collider. Phys. Rev. D **63**, 075007 (2001). arXiv:hep-ph/0011332
43. S. Baek, D.K. Ghosh, X.-G. He, W.-Y.P. Hwang, Signatures of noncommutative QED at photon colliders. Phys. Rev. D **64**, 056001 (2001). arXiv:hep-ph/0103068
44. J.L. Hewett, F.J. Petriello, T.G. Rizzo, Signals for noncommutative interactions at linear colliders. Phys. Rev. D **64**, 075012 (2001). arXiv:hep-ph/0010354
45. S. Godfrey, M.A. Doncheski, Signals for noncommutative QED in $e\gamma$ and $\gamma\gamma$ collisions. Phys. Rev. D **65**, 015005 (2001). arXiv:hep-ph/0108268
46. T.G. Rizzo, Signals for noncommutative QED at future e^+e^- colliders. Int. J. Mod. Phys. A **18**, 2797 (2003). arXiv:hep-ph/0203240
47. T. Ohl, J. Reuter, Testing the noncommutative standard model at a future photon collider. Phys. Rev. D **70**, 076007 (2004). arXiv:hep-ph/0406098
48. R. Horvat, D. Latas, J. Trampetić, J. You, Light-by-light scattering and spacetime noncommutativity. Phys. Rev. D **101**, 095035 (2020). arXiv:2002.01829
49. D. Latas, J. Trampetić, J. You, Seiberg–Witten map invariant scatterings. Phys. Rev. D **104**, 015021 (2021). arXiv:2012.07891
50. ATLAS Collaboration, ATLAS forward detectors for measurement of elastic scattering and luminosity. CERN-LHCC-2008-004, ATLAS-TDR-18
51. S. Abdel Khalek et al., The ALFA Roman Pot detectors of ATLAS. JINST **11**, P11013 (2016)
52. ATLAS Collaboration, Letter of intent for the phase-I upgrade of the ATLAS experiment. Technical Report. CERN-LHCC-2011-012. LHCC-I-020, November (2011)
53. L. Adamczyk et al., Technical design report for the ATLAS forward proton detector. Technical Report. CERN-LHCC-2015-009. ATLAS-TDR-024 (2015)
54. M. Albrow et al., CMS-TOTEM precision proton spectrometer CMS-TOTEM. Technical Report. CERN-LHCC-2014-021; TOTEM-TDR-003; CMS-TDR-13 (2014)
55. G. Antchev et al. (TOTEM Collaboration), First measurement of the total proton-proton cross-section at the LHC energy of $\sqrt{s} =$ 7 TeV. EPL **96**, 21002 (2011)
56. G. Antchev et al. (TOTEM Collaboration), Measurement of the forward charged-particle pseudorapidity density in pp collisions at $\sqrt{s}$ = 7 TeV with the TOTEM experiment. EPL **98**, 31002 (2012)
57. G. Antchev et al. (TOTEM Collaboration), Measurement of proton–proton elastic scattering and total cross-section at $\sqrt{s} =$ 7 TeV. EPL **101**, 21002 (2013)
58. M.G. Albrow et al., The FP420 R&D project: Higgs and new physics with forward protons at the LHC. JINST **4**, T10001 (2009). arXiv:0806.0302
59. M.G. Albrow et al., Forward physics with rapidity gaps at the LHC. JINST **4**, P10001 (2009). arXiv:0811.0120
60. M.G. Albrow, T.D. Coughlin, J.R. Forshaw, Central exclusive particle production at high energy hadron colliders. Prog. Part. Nucl. Phys. **65**, 149 (2010). arXiv:1006.1289
61. İ Şahin, S.C. İnan, Probe of unparticles at the LHC in exclusive two lepton and two photon production via photon–photon fusion. JHEP **09**, 069 (2009). arXiv:0907.3290
62. S.C. İnan, Exclusive excited leptons search in two lepton final states at the CERN LHC. Phys. Rev. D **81**, 115002 (2010). arXiv:1005.3432
63. S. Atağ, S.C. İnan, İ Şahin, Extra dimensions in $\gamma\gamma \to \gamma\gamma$ process at the CERN-LHC. JHEP **09**, 042 (2010). arXiv:1005.4792
64. İ Şahin, A.A. Billur, Anomalous $WW\gamma$ couplings in γp collision at the LHC. Phys. Rev. D **83**, 035011 (2011). arXiv:1101.4998
65. İ Şahin, M. Köksal, Search for electromagnetic properties of the neutrinos at the LHC. JHEP **03**, 100 (2011). arXiv:1010.3434
66. S.C. İnan, A.A. Billur, Polarized top pair production in extra dimension models via photon–photon fusion at the CERN LHC. Phys. Rev. D **84**, 095002 (2011)
67. R.S. Gupta, Probing quartic neutral gauge boson couplings using diffractive photon fusion at the LHC. Phys. Rev. D **85**, 014006 (2012). arXiv:1111.3354
68. İ Şahin, Electromagnetic properties of the neutrinos in γp collision at the LHC. Phys. Rev. D **85**, 033002 (2012). arXiv:1201.4364
69. A.A. Billur, Anomalous top-gluon couplings in γp collision at the CERN-LHC. EPL **101**, 21001 (2013)
70. İ Şahin et al., Probe of extra dimensions in $\gamma q \to \gamma q$ at the LHC. Phys. Rev. D **88**, 095016 (2013). arXiv:1304.5737
71. H. Sun, C.X. Yue, Precise photoproduction of the charged top-pions at the LHC with forward detector acceptances. Eur. Phys. J. C **74**, 2823 (2014). arXiv:1401.0250
72. H. Sun, Probe anomalous $tq\gamma$ couplings through single top photoproduction at the LHC. Nucl. Phys. B **886**, 691 (2014). arXiv:1402.1817
73. S. Fichet, G. von Gersdorff, B. Lenzi et al., Light-by-light scattering with intact protons at the LHC: from standard model to new physics. JHEP **02**, 165 (2015). arXiv:1411.6629
74. İ Şahin et al., Graviton production through photon-quark scattering at the LHC. Phys. Rev. D **91**, 035017 (2015). arXiv:1409.1796
75. S. Fichet, G. von Gersdorff, C. Royon, Measuring the diphoton coupling of a 750 GeV resonance. Phys. Rev. Lett. **116**, 231801 (2016). arXiv:1601.01712
76. S. Fichet, G. von Gersdorff, C. Royon, Scattering light by light at 750 GeV at the LHC. Phys. Rev. D **93**, 075031 (2016). arXiv:1512.05751
77. S. Fichet, Shining light on polarizable dark particles. JHEP **04**, 088 (2017). arXiv:1609.01762
78. C. Baldenegro, S. Fichet, G. von Gersdorff, C. Royon, Probing the anomalous $\gamma\gamma\gamma Z$ coupling at the LHC with proton tagging. JHEP **06**, 142 (2017). arXiv:1703.10600
79. C. Baldenegro, S. Fichet, G. von Gersdorff, C. Royon, Searching for axion-like particles with proton tagging at the LHC. JHEP **06**, 131 (2018). arXiv:1803.10835
80. M. Köksal et al., Analysis of the anomalous electromagnetic moments of the tau lepton in γp collisions at the LHC. Phys. Lett. B **783**, 375 (2018). arXiv:1711.02405
81. S.C. İnan, A.V. Kisselev, Search for the RS model with a small curvature through photon-induced process at the LHC. Eur. Phys. J. C **78**, 729 (2018). arXiv:1805.01441
82. S.C. İnan, A.V. Kisselev, Probe of the Randall–Sundrum-like model with the small curvature via light-by-light scattering at the LHC. Phys. Rev. D **100**, 095004 (2019). arXiv:1902.08615
83. H. Terazawa, Two-photon processes for particle production at high energies. Rev. Mod. Phys. **45**, 615 (1973)
84. V. Budnev, I. Ginzburg, G. Meledin, V. Serbo, The two-photon particle production mechanism. Physical problems. Applications. Equivalent photon approximation. Phys. Rep. **15**, 181 (1975)
85. G. Baur et al., Coherent $\gamma\gamma$ and γA interactions in very peripheral collisions at relativistic ion colliders. Phys. Rep. **364**, 359 (2002). arXiv:hep-ph/0112211
86. J.-H. Huang, R. Huang, Y. Jia, Tree amplitudes of noncommutative $U(N)$ Yang–Mills theory. J. Phys. A: Math. Theor. **44**, 425401 (2011). arXiv:1009.5073
87. P.A. Zyla et al. (Particle Data Group), Prog. Theor. Exp. Phys. **2020**, 083C01 (2020)

88. ATLAS Collaboration, Observation and measurement of forward proton scattering in association with lepton pairs produced via the photon fusion mechanism at ATLAS. Phys. Rev. Lett. **125**, 261801 (2020). arXiv:2009.14537
89. CMS and TOTEM Collaborations, First search for exclusive diphoton production at high mass with tagged protons in proton–proton collisions at $\sqrt{s} = 13$ TeV. Phys. Rev. Lett. **129**, 011801 (2022). arXiv:2110.05916
90. C. Baldenegro, S. Fichet, G. von Gersdorff, C. Royon, Searching for axion-like particles with proton tagging at the LHC. JHEP **06**, 131 (2018). arXiv:1803.10835
91. X.-A. Pan et al., Photoproduction of the double J/ψ (Υ) at the LHC with forward proton tagging. Phys. Rev. D **99**, 014029 (2019). arXiv:1812.08599
92. C. Royon, Anomalous coupling studies with proton tagging at the LHC. Acta Phys. Pol. B Proc. Suppl. **12**, 805 (2019)
93. L.A. Harland-Lang, V.A. Khoze, M.G. Ryskin, M. Tasevsky, LHC searches for dark matter in compressed mass scenarios: challenges in the forward proton mode. JHEP **04**, 010 (2019). arXiv:1812.04886
94. G.-C. Cho, K. Yamashita, M. Yonemura, Search for vector-mediated dark matter at the LHC with forward proton tagging. Phys. Rev. D **101**, 035018 (2020). arXiv:1908.06357
95. V.P. Gonçalves, D.E. Martins, M.S. Rangel, Diffractive $\gamma\gamma$ production in pp collisions at the LHC. Eur. Phys. J. C **80**, 841 (2020)
96. C. Baldenegro, G. Biagi, G. Legras, C. Royon, Central exclusive production of W boson pairs in pp collisions at the LHC in hadronic and semi-leptonic final states. JHEP **12**, 165 (2020). arXiv:2009.08331
97. R. Karplus, M. Neuman, The scattering of light by light. Phys. Rev. **83**, 776 (1951)
98. V. Costantini, B. De Tollis, G. Pistoni, Nonlinear effects in quantum electrodynamics. Nuovo Cim. A **2**, 733 (1971)
99. G. Jikia, A. Tkabladze, Photon–photon scattering at the photon linear collider. Phys. Lett. B **323**, 453 (1994). arXiv:hep-ph/9312228
100. G.J. Gounaris, P.I. Porfyriadis, F.M. Renard, Light by light scattering at high energy: a tool to reveal new particles. Phys. Lett. B **452**, 76 (1999). arXiv:hep-ph/9812378. [Erratum, ibid. **513**, 431 (2001)]
101. G.J. Gounaris, P.I. Porfyriadis, F.M. Renard, The gamma gamma to gamma gamma process in the Standard and SUSY models at high energies. Eur. Phys. J. C **9**, 673 (1999). arXiv:hep-ph/9902230
102. S.C. İnan, A.V. Kisselev, A search for axion-like particles in light-by-light scattering at the CLIC. JHEP **06**, 183 (2020). arXiv:2003.01978
103. G. Cowan, K. Cranmer, E. Gross, O. Vitells, Asymptotic formulae for likelihood-based tests of new physics. Eur. Phys. J. C **71**, 1554 (2011). arXiv:1007.1727. [Erratum ibid. **73**, 2501 (2013)]
104. S. Minwalla, M. Van Raamsdonk, N. Seiberg, Noncommutative perturbative dynamics. JHEP **02**, 020 (2000). arXiv:hep-th/9912072
105. K.B. Eom et al., Radiative corrections in noncommutative QED. arXiv:hep-th/0205093
106. P. Schupp, J. You, UV/IR mixing in noncommutative QED defined by Seiberg–Witten map. JHEP **08**, 107 (2008). arXiv:0807.4886